Eur. Phys. J. D **7**, 279–284 (1999)

THE EUROPEAN PHYSICAL JOURNAL D

EDP Sciences

Exotic quantum dark states

S. Kulin[a], Y. Castin[b], M. Ol'shanii[c], E. Peik[d], B. Saubaméa, M. Leduc, and C. Cohen-Tannoudji

Collège de France and Laboratoire Kastler Brossel, École Normale Supérieure, 24 rue Lhomond, 75231 Paris Cedex 05, France

Received 18 December 1998 and Received in final form 29 January 1999

Abstract. We extend studies of velocity selective coherent population trapping to atoms having a $J = 1 \rightarrow J = 0$ transition. When placed in a two-dimensional laser field these atoms are optically pumped into different velocity selective nonabsorbing states. Each of these distinct energy eigenstates exhibits a unique entanglement between its internal and external degrees of freedom. We use a graphical method that makes easier the description of these states. We confirm our predictions experimentally.

PACS. 32.80.Pj Optical cooling of atoms; trapping – 34.50.Rk Laser-modified scattering and reactions – 42.50.Vk Mechanical effects of light on atoms, molecules, electrons, and ions

1 Introduction

Laser cooling and trapping techniques allow the creation of a sample of atoms or ions in well-specified states. The selection of atoms in the lowest vibrational state in a far detuned optical lattice [1] and the ion crystal in a radiofrequency trap are two examples [2,3]. Velocity selective coherent population trapping (VSCPT) is a manner of preparing atoms in stationary states of very well-defined momentum in which the atoms do not absorb photons ("dark states"). To date VSCPT has been studied in detail on the $J = 1 \rightarrow J = 1$ transition in both helium and rubidium [4–10]. In this case there exists a dark state that is isomorphic to the laser field [5,6]. Exploiting the coherence properties of this state has led to a series of interesting experiments [11,12].

It is then natural to inquire about the existence of dark states on transitions other than $J \rightarrow J$. It is well-known, that a $J \rightarrow J+1$ transition is a "cycling" transition and does not support nonabsorbing states. On the other hand, a $J \rightarrow J-1$ transition does allow non-coupled states [13,14]. The simplest $J \rightarrow J-1$ transition is the $1 \rightarrow 0$ transition, which is the one we study here. For instance, light polarized σ_+ pumps the atoms into both the $|g_0\rangle$ and $|g_{+1}\rangle$ ground states, where they no longer absorb photons. But in a one-dimensional light field these non-coupled states are not velocity selective, and thus not of interest to us. In this work, we discuss the existence and the nature of velocity selective dark states on the $J = 1 \rightarrow J = 0$ transition in the presence of a two-dimensional light field. As opposed to the case of the $J = 1 \rightarrow J = 1$ transition, several dark states appear at different energies. These issues have been addressed theoretically in [5,13,15]. Here, we choose to use the cooling scheme of [5], the simplest one to implement experimentally. We use a graphical analysis inspired by that introduced in [5,13,16] that allows us to determine the minimal number of dark states that we can populate in each energy class, taking into account solely the symmetry of the laser field and the atomic transition. We then compare these predictions with the experimental results.

2 Characterization of dark states

The idea of VSCPT is to optically pump the atoms into states $|\Psi\rangle$ where they can remain indefinitely without scattering any photons. We can thus characterize such dark states by two conditions: first, they have to be decoupled from the light, and second, they must be stationary.

Mathematically, the condition for a non-coupled state is expressed by requiring that the transition amplitude $\mathcal{A}$ from a ground state $|\Psi\rangle$ to the excited state $|\Phi\rangle$ *via* the atom-laser interaction potential vanishes:

$$\mathcal{A} = \langle \Phi | V_{\mathrm{AL}} | \Psi \rangle = 0, \quad \forall \ |\Phi\rangle \,. \tag{1}$$

Here, following the notation of [17], $V_{\mathrm{AL}} = -\mathbf{d} \cdot \mathbf{E}_{\mathrm{L}}(\mathbf{r})$, with $\mathbf{d}$ the raising dipole moment operator and $\mathbf{E}_{\mathrm{L}}(\mathbf{r})$ the positive frequency part of the electric field of the laser at the position $\mathbf{r}$ of the atom. The most general ground state $|\Psi\rangle$ is a superposition of all three Zeeman sublevels

[a] *Present address*: National Institute of Standards and Technology, Gaithersburg, MD 20899-8424, USA.

[b] e-mail: `castin@physique.ens.fr`

[c] *Present address*: Lyman Laboratory, Physics Department Harvard University, Cambridge, MA 02138, USA.

[d] *Present address*: Max Planck Institut für Quantenoptik, Hans Kopfermann Straße 1, 85748 Garching, Germany.

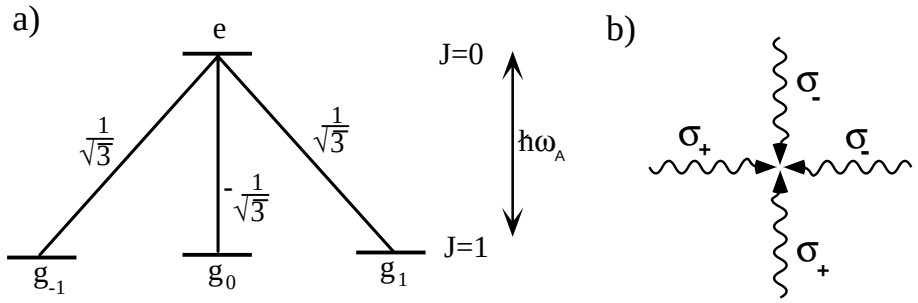

Fig. 1. The atomic transition and the laser field. (a) The $J = 1 \rightarrow J = 0$ transition and the corresponding Clebsch-Gordan coefficients. (b) The laser field consists of two standing waves each polarized σ_+ and σ_- and oriented along the x and y axis, respectively.

and can be viewed as a vector field $\boldsymbol{\Psi}(\mathbf{r})$. Projecting out the magnetic quantum number, the following one-to-one mapping between the position space wavefunction $|\Psi(\mathbf{r})\rangle$ and the vector field $\boldsymbol{\Psi}(\mathbf{r})$ can be established:

$$|\Psi(\mathbf{r})\rangle = \sum_{m=0,\pm1} \langle m, \mathbf{r}|\Psi\rangle \, |m\rangle \longleftrightarrow \boldsymbol{\Psi}(\mathbf{r}) = \sum_{m=0,\pm1} \langle m, \mathbf{r}|\Psi\rangle \, \mathbf{e}_m \,,$$

where $|m\rangle$ are the Zeeman ground state sublevels (see Fig. 1a), and $\mathbf{e}_m$ are the unit vectors in the spherical basis. By using the Clebsch-Gordan coefficients of the $J = 1 \rightarrow J = 0$ transition (see Fig. 1a) and by choosing a Cartesian basis in configuration space, equation (1) yields, as shown in [13]:

$$\mathcal{A} = \frac{\mathcal{D}}{\sqrt{3}} \int \mathrm{d}^3 r \, \Phi^*(\mathbf{r}) \, (\mathbf{E}_\mathrm{L}(\mathbf{r}) \cdot \boldsymbol{\Psi}(\mathbf{r})) = 0 \,, \qquad (2)$$

where $\mathcal{D}$ is the reduced dipole matrix element. When $\mathcal{A} = 0$, the transition amplitudes from all ground state Zeeman sublevels to the excited state interfere destructively. This condition must be satisfied for every $\Phi(\mathbf{r})$, and therefore equation (2) imposes $\mathbf{E}_\mathrm{L}(\mathbf{r}) \cdot \boldsymbol{\Psi}(\mathbf{r}) = 0$. For this atomic transition a non-coupled state is always orthogonal to the laser field. This situation is fundamentally different from the case of a $J = 1 \rightarrow J = 1$ transition, where the dark state is always aligned with the laser field, because in the expression of $\mathcal{A}$ the cross product then appears instead of the dot product [6,16].

In order to be a dark state, $\boldsymbol{\Psi}$ must also be an eigenstate of the total Hamiltonian, which in this case consists of two terms: the kinetic energy operator $\mathbf{P}^2/2M$ (where M is the mass) and the atom laser interaction Hamiltonian V_AL. Since for any non-coupled state the second part vanishes, the eigenstates of the Hamiltonian are eigenstates of the kinetic energy operator $(\hbar^2\Delta/2M)\boldsymbol{\Psi} = E\boldsymbol{\Psi}$. Therefore, all ground state sublevels of a dark state need to have the same energy, or equivalently the same modulus of the momentum.

3 Graphical method for finding dark states

With the general considerations of the previous section in mind, and following graphical methods similar to those of [5,13,16], we now develop a formalism that will allow us to determine for which energies dark states exist, and their degeneracies, when cooling atoms in the two-dimensional light field sketched in Figure 1b. All Zeeman ground state sublevels that might participate in forming a dark state must have the same momentum $p = (p_x^2 + p_y^2)^{1/2}$. Under the influence of the atom-laser coupling any change of p_x and p_y occurs in steps of $\hbar k$, the photon momentum. An atom can only suffer stimulated emission or absorption of photons from one of the four laser waves at a time. This implies that the different states that can be coupled *via* absorption or induced emission lie on a grid in momentum space. The unit cell of this grid is exactly $\hbar k \times \hbar k$.

Thus, a dark state is a superposition of ground state sublevels with momenta both on a circle of radius p and on a grid of step size $\hbar k$. We therefore have to consider a geometric problem: the number of intersections between a circle of radius p and a grid of step size $\hbar k$. In what follows we set the origin of the grid at $p_x = 0$, $p_y = 0$. In order for destructive interference to take place, an excited state has to be reached from different ground state levels. The differences in momenta between the ground state sublevels become subject to constraints.

In momentum space, the smallest circle that intersects the grid has a radius equal to $\hbar k$. For simplicity, from now on we express the components p_x and p_y in units of $\hbar k$. The four possible intersections occur at coordinates $(\pm1, 0)$ and $(0, \pm1)$ in momentum space. A dark state with energy $E = E_\mathrm{rec} = \hbar^2 k^2/2M$ can be constructed out of ground state sublevels having momenta in these points of the $p_x - p_y$ plane. The situation is shown in Figure 2. Any one of the crosses can represent either one of the three ground state sublevels. This yields 4×3 possibilities for the states represented by a cross. It is convenient to denote Ψ_{n_x,n_y} the wavefunction associated with the momentum state $(p_x = n_x\hbar k, p_y = n_y\hbar k)$. Let us now consider for example the ground state at $(+1, 0)$ described by the wavefunction $\Psi_{1,0}$.When absorbing a photon from the light wave that propagates along the x axis in the positive direction, the atom ends in the excited state with coordinates $(2, 0)$. Since this state cannot be attained from any of the other ground states $\Psi_{0,1}$, $\Psi_{-1,0}$, $\Psi_{0,-1}$ by absorption of a single photon, destructive interference cannot take place. The condition that $|e, p_x = 2\hbar k, p_y = 0\rangle$ should not be

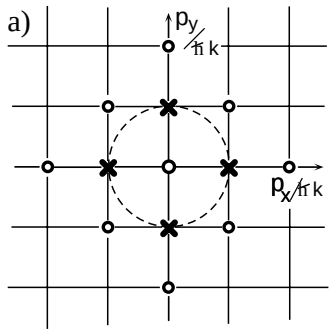

b)

Possible states:	12
Constraints:	4
Interference cond. :	5
Minimum number of dark states:	**3**

Fig. 2. Dark states of energy $E = E_{\rm rec}$. (a) The $(p_x/\hbar k) - (p_y/\hbar k)$ plane in momentum space is divided into cells of size 1×1. The "crosses" representing ground states are arranged on a circle of radius 1. The circles mark the excited states that can be attained from the ground states by one step of size 1. (b) Table summarizing the graphical analysis.

excited by the laser light places a constraint on the internal state in which the atom at $(1, 0)$ can be. For instance consider the case in which the laser wave that propagates in the positive direction along the x axis is polarized σ_+. According to the above reasoning the internal state of the wavefunction $\Psi_{1,0}$ cannot be $|g_{-1}\rangle$. Similarly, we deduce a constraint for each one of the other states $\Psi_{0,1}$, $\Psi_{-1,0}$, $\Psi_{0,-1}$. We thus eliminate one (out of three) ground state sublevels for every possible ground state. This reduces the number of possible "cross"-states from twelve to eight.

We now return to the state $\Psi_{1,0}$. By absorbing a photon from the laser wave that propagates in the positive direction along the y axis, it passes into the excited state with coordinates $(1, 1)$. This state can also be reached by absorption of one photon from the state $\Psi_{0,1}$. Therefore, destructive interference between the two transition amplitudes from $\Psi_{1,0}$ and $\Psi_{0,1}$ can, in principle, take place. We thus obtain an equation that involves these two ground states and expresses the destructive interference condition. The same argument leads to three further equations, each involving two of the four states marked by a cross in Figure 2.

Finally, a third way for an atom to reach an excited state starting from $\Psi_{1,0}$ is to absorb a photon from the laser wave that propagates along the Ox axis in the negative direction. This excited state of coordinates $(0, 0)$ can also be attained from the states $\Psi_{0,1}$, $\Psi_{-1,0}$, $\Psi_{0,-1}$. The condition for destructive interference involving all transition amplitudes leads to a fifth equation.

To summarize, we now have eight unknowns and $5 = 4 + 1$ equations to determine the internal states of the wavefunctions $\Psi_{1,0}$, $\Psi_{0,1}$, $\Psi_{-1,0}$, and $\Psi_{0,-1}$ that can contribute to the construction of the dark states. From this we deduce that there exist at least three solutions that are dark states of energy $E = E_{\rm rec}$ (see also table next to Fig. 2).

Note that the number of possible ground states is given by the number of crosses in Figure 2 multiplied by 3. The number of circles is equal to the sum of constraints and interference conditions. The minimum number of dark states that exist for a given energy is just the difference between these two numbers.

According to the above considerations we can calculate analytically the explicit form of the dark states of energy $E = E_{\rm rec}$. The laser field $\mathbf{E}_{\rm L}(\mathbf{r})$ that we use for cooling consists of two orthogonally oriented standing waves $\mathbf{E}_1(\mathbf{r})$ and $\mathbf{E}_2(\mathbf{r})$. Each standing wave is formed by two counterpropagating laser waves of equal amplitude $\mathcal{E}_0$ and polarized σ_+ and σ_- respectively. The total electric field will thus be $\mathbf{E}_{\rm L}(\mathbf{r}) = \mathbf{E}_1(\mathbf{r}) + \mathbf{E}_2(\mathbf{r})\mathrm{e}^{\mathrm{i}\phi}$, where ϕ is the relative phase between the two standing waves. To be specific we choose the origin of coordinates along the x axis and the y axis so that the standing waves, assumed for simplicity to have the same intensity, have the following spatial dependence:

$$\mathbf{E}_1(\mathbf{r}) = -\frac{\mathcal{E}_0}{\sqrt{2}}(\mathbf{e}_y + \mathrm{i}\mathbf{e}_z)\mathrm{e}^{\mathrm{i}kx} + \frac{\mathcal{E}_0}{\sqrt{2}}(\mathbf{e}_y - \mathrm{i}\mathbf{e}_z)\mathrm{e}^{-\mathrm{i}kx}, \quad (3)$$

$$\mathbf{E}_2(\mathbf{r}) = -\frac{\mathcal{E}_0}{\sqrt{2}}(\mathbf{e}_z + \mathrm{i}\mathbf{e}_x)\mathrm{e}^{\mathrm{i}ky} + \frac{\mathcal{E}_0}{\sqrt{2}}(\mathbf{e}_z - \mathrm{i}\mathbf{e}_x)\mathrm{e}^{-\mathrm{i}ky}. \quad (4)$$

It is at this point more convenient to use Cartesian coordinates to describe the ground state sublevels $|g_x\rangle$, $|g_y\rangle$, $|g_z\rangle$ and accordingly the vector field $\boldsymbol{\Psi}(\mathbf{r})$ that we use to describe the state $|\Psi\rangle$ (see also Eq. (2)).

Solving the system of equations that comprises the constraints and destructive interference conditions leads indeed to three solutions [18]. The vectors associated with the dark states are given by:

$$\begin{cases} \boldsymbol{\Psi}_1(\mathbf{r}) = \mathbf{e}_x \times \mathbf{E}_{\rm L}(\mathbf{r}) \\ \boldsymbol{\Psi}_2(\mathbf{r}) = \mathbf{e}_y \times \mathbf{E}_{\rm L}(\mathbf{r}). \\ \boldsymbol{\Psi}_3(\mathbf{r}) = \mathbf{e}_z \times \mathbf{E}_{\rm L}(\mathbf{r}) \end{cases} \quad (5)$$

It is easily verified that these states are both not coupled to the excited state and eigenstates of the kinetic energy operator as $(\Delta + k^2)\mathbf{E}_{\rm L}(\mathbf{r}) = 0$. To clarify the structure of these dark states, we now concentrate on the state $\boldsymbol{\Psi}_1(\mathbf{r})$. The vector product in equation (5) reduces the number of ground state sublevels involved to two: $\mathbf{e}_y$ and $\mathbf{e}_z$, or equivalently $|g_y\rangle$ and $|g_z\rangle$. As for the external degrees of freedom the state has four momentum components, corresponding to the different wavevectors $\pm k\mathbf{e}_x$ and $\pm k\mathbf{e}_y$ of the laser field. In position representation equation (5) can be rewritten as:

$$|\Psi_1(\mathbf{r})\rangle = \frac{\mathcal{E}_0}{\sqrt{2}}\left(|g_z\rangle(\mathrm{e}^{-\mathrm{i}kx} - \mathrm{e}^{\mathrm{i}kx}) + |g_y\rangle(\mathrm{i}\mathrm{e}^{\mathrm{i}kx} + \mathrm{i}\mathrm{e}^{-\mathrm{i}kx} + \mathrm{e}^{\mathrm{i}ky}\mathrm{e}^{\mathrm{i}\phi} - \mathrm{e}^{-\mathrm{i}ky}\mathrm{e}^{\mathrm{i}\phi})\right). \quad (6)$$

Note that a given internal state can be associated with several external states. The other two dark states $|\Psi_2\rangle$ and $|\Psi_3\rangle$ have similar structures, each of them involving two ground state sublevels and having the same four components in momentum space. Experimentally, we can only access the external degrees of freedom. Since all dark states are localized at the same points in momentum space, at $(\pm\hbar k, 0)$ and $(0, \pm\hbar k)$, we cannot distinguish between the three states.

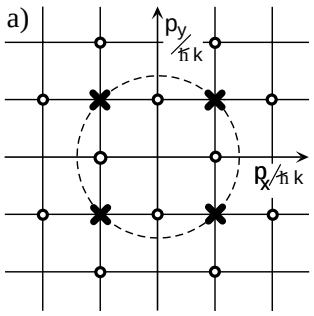

b)

Possible states:	12
Constraints:	8
Interference cond. :	4
Minimum number of dark states:	**0**

Fig. 3. Dark states with energy $E = 2E_{\rm rec}$. (a) The states able to form such a dark state are represented by a cross. (b) The table indicates the number of possible states that can form the dark state, as well as the number of constraints and destructive interference conditions that need to be satisfied.

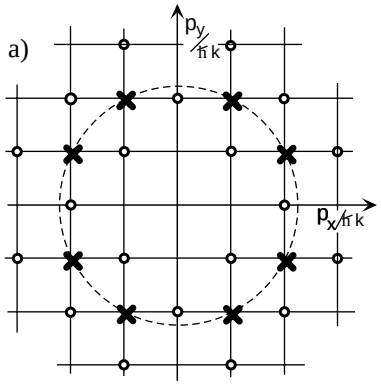

b)

Possible states:	24
Constraints:	8
Interference cond. :	12
Minimum number of dark states:	**4**

Fig. 4. Dark states with energy $E = 5E_{\rm rec}$. (a) The distribution of ground states in momentum space. (b) Summary of the number of possible states and equations to be satisfied for the dark state.

The graphical method we presented above is easily extended to other energy classes and allows us to predict other dark states that may be populated when cooling in two dimensions by VSCPT on a $J = 1 \rightarrow J = 0$ transition. We shall now illustrate this for the next higher lying energy $E = 2E_{\rm rec}$. Figure 3 schematically shows the possible locations in momentum space of the ground state sublevels. We distinguish four intersections between the grid in p-space and the "energy"-circle of radius $\sqrt{2}\hbar k$. The above reasoning in terms of constraints and destructive interference conditions is summarized in the table next to Figure 3. It suffices to multiply the number of crosses by three and subtract the number of circles on the graph, in order to determine a minimal number of dark states with energy $E = 2E_{\rm rec}$. This difference vanishes. It is therefore not clear whether or not there exists a dark state in this case. Nevertheless, when solving the system of equations obtained one finds that there exists one dark state. The vector assigned to this state is given by:

$$\boldsymbol{\Psi}(\mathbf{r}) = \mathbf{E}_1(\mathbf{r}) \times \mathbf{E}_2(\mathbf{r}). \tag{7}$$

A closer look at this equation reveals that the dark state is a superposition of all three ground state sublevels $|g_x\rangle$, $|g_y\rangle$ and $|g_z\rangle$, each being associated with several different momentum states corresponding to the crosses in Figure 3.

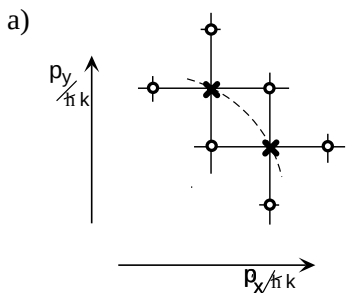

b)

Possible states:	6
Constraints:	4
Interference cond. :	2
Minimum number of dark states:	**0**

Fig. 5. Disposition of isolated pairs in the plane $(p_x/\hbar k) - (p_y/\hbar k)$ in momentum space that appear when looking for intersections between the circles of radii larger than $\sqrt{5}$.

A natural question at this point is whether or not there exist dark states of even higher energy $E = nE_{\rm rec}$ with $n > 2$. Geometrically, when increasing the radius of the circle on which the Zeeman ground state sublevels lie, the intersections with the grid in momentum space form an octagon for $n = 5$, and for higher n the crossings become either isolated points or form pairs of the type shown in Figure 5. The octagon is shown in Figure 4. The coordinates (x, y) of the vertices are such that $x, y \in \{\pm 1, \pm 2, |x| \neq |y|\}$, in units of $\hbar k$. From the table next to the graph we infer that there exist at least four dark states having an energy $E = 5E_{\rm rec}$. For this case we do not know the analytic expressions of the dark states. Nevertheless, the graphical method allows us to anticipate the experimental results: we expect to see eight wavepackets placed on a circle of radius $\sqrt{2^2 + 1^2}$ in momentum space.

By an "isolated" point in momentum space we mean a ground state sublevel not connected *via* absorption of a single photon to an excited state coupled to another ground state. The graphical method shows that such an isolated "cross" in momentum space is not a candidate for a dark state. The three ground state sublevels would have to obey four constraints simultaneously.

Finally, consider the last case mentioned above where the crossings form isolated pairs (Fig. 5). Each of the two ground state momentum components of the pair must be coupled by a single photon absorption to a common excited state momentum component, in order to obtain destructive interference. We label the two momentum components in the ground state by (n_x, n_y) and $(n_x{+}1, n_y{\pm}1)$, n_x corresponding to the smallest momentum component along x. The fact that these two states belong to the same circle in momentum space can be expressed mathematically by the following relation:

$$n_x^2 + n_y^2 = (n_x + 1)^2 + (n_y \pm 1)^2. \tag{8}$$

This equation leads to $n_x \pm n_y + 1 = 0$. Applying the graphical method in terms of constraints and destructive interference conditions to this pair of cross-points we cannot know whether there exists a dark state. However, the analytic solution shows, that in general there is no dark

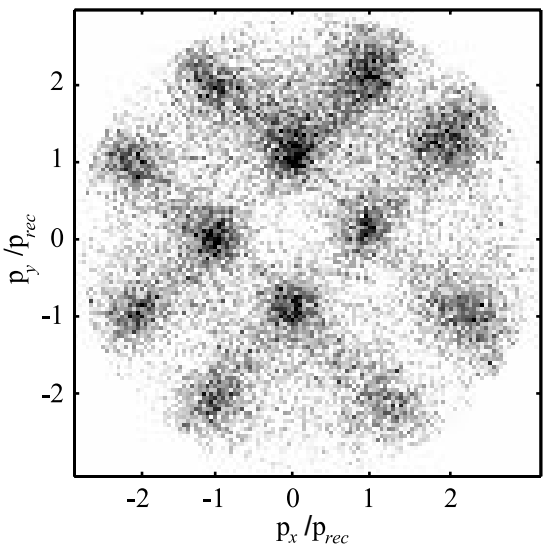

Fig. 6. Measured distribution of the atomic momenta after an interaction time of 1 ms with the laser tuned to the $2^3S_1 \rightarrow 2^3P_0$ transition in helium (Rabi frequency $\Omega = \Gamma$, detuning $\delta = +1\Gamma$). In the plane $(p_x/p_{\rm rec}) - (p_y/p_{\rm rec})$ in momentum space (where $p_{\rm rec} = \hbar k$) we distinguish four wavepackets that lie on a circle of radius 1 and eight wavepackets located at ($p_x/p_{\rm rec} = \pm 2$, $p_y/p_{\rm rec} = \pm 1$) and ($p_x/p_{\rm rec} = \pm 1$, $p_y/p_{\rm rec} = \pm 2$). The figure is an integration of 50 consecutive experiments.

state that corresponds to such an arrangement of ground state sublevels in momentum space [19]. We therefore conclude, that $E = 5\,E_{\rm rec}$ is the highest energy a dark state can have in a two-dimensional laser field configuration.

4 Experimental results

In the experiment we start with a sample of about 10^5 metastable helium atoms that we prepare in a magneto-optical trap [20,21] to have a momentum distribution centered around zero with a width of approximately $5\,\hbar k$. The atoms are then released from the trap and immediately interact with light tuned to the $2^3S_1 \rightarrow 2^3P_0$ transition. After typically 1 ms of interaction time, the light is turned off and the atoms fall onto a position sensitive detector located 6.8 cm below. The detector also registers the arrival time of the atoms. Assuming a point source, from both position and temporal information we then compute the velocity (or the momentum) the atoms had at the end of the interaction time.

Figure 6 shows the momentum distribution of the atoms that we measure in such an experiment. One distinguishes four wavepackets that appear at a distance $p_{\rm rec} = \hbar k$ from the center. In addition one counts eight spots that are located around the points of coordinates ($p_x = \pm 2\,p_{\rm rec}$, $p_y = \pm 1\,p_{\rm rec}$) and ($p_x = \pm 1\,p_{\rm rec}$, $p_y = \pm 2\,p_{\rm rec}$) on a circle at the border of the image. We thus observe the dark states associated with the energies $E = 1E_{\rm rec}$ and $E = 5E_{\rm rec}$.

According to the previous discussion, we would expect to also see the dark states that have an energy $E = 2E_{\rm rec}$. Numerical calculations of the energy band structure [22] show that the regions in velocity space for which the photon absorption is inhibited (the "Raman holes") have different widths for the various energy classes. While the Raman holes centered at the states with energy $E = 1E_{\rm rec}$ and $E = 5E_{\rm rec}$ have comparable widths, the width of the Raman hole at $E = 2E_{\rm rec}$ is approximately five times narrower. Since all the states are populated by spontaneous emission, this suggests that the efficiency of the cooling is related to the width of these holes and could explain why we do not observe the dark states associated to the energy of $E = 2E_{\rm rec}$ in the experiment.

5 Conclusion

In conclusion, we have shown that the $J = 1 \rightarrow J = 0$ transition supports a large number of velocity selective dark resonances. Thanks to a graphical method we have shown in a simple way that for two-dimensional light field there exist several dark states belonging to different energy classes ($1E_{\rm rec}$, $2E_{\rm rec}$, $5E_{\rm rec}$). Using symmetry arguments we could deduce the minimum number of states that exist for a given energy. Finally, we performed an experiment in which we observed for the first time such dark states. A number of theoretical and experimental issues, like for instance the relative filling factors of the states in different energy classes or the coherence properties of the states, remain to be investigated and could lead to interesting further insights and future experiments.

We thank very much Ralph Dum for his contribution with the numerical band structure calculations of energies and excitation probabilities. We greatly appreciate discussions with T. Hijmans and J. Lawall, and thank E. Rasel for help with the experiment. Simone Kulin acknowledges support from the DAAD and the Alexander von Humboldt Foundation. Laboratoire Kastler Brossel is a Laboratoire de l'ENS et de l'Université Paris VI, associé au CNRS.

References

1. T. Müller-Seydlitz, M. Hartl, B. Brezger, H. Hänsel, C. Keller, A. Schnetz, R. Spreeuw, T. Pfau, J. Mlynek, Phys. Rev. Lett. **78**, 4011 (1997).
2. F. Diedrich, E. Peik, J.M. Chen, W. Quint, H. Walther, Phys. Rev. Lett. **59**, 2931 (1987).
3. D.J. Wineland, J.C. Bergquist, W.M. Itano, J.J. Bollinger, C.H. Manney, Phys. Rev. Lett. **59**, 2935 (1987).
4. A. Aspect, E. Arimondo, R. Kaiser, N. Vansteenkiste, C. Cohen-Tannoudji, Phys. Rev. Lett. **61**, 826 (1988).
5. M.A. Ol'shanii, V.G. Minogin, in *Light Induced Kinetic Effects on Atoms, Ions and Molecules*, edited by L. Moi, S. Gozzini, C. Gabbanini, E. Arimondo, F. Strumia (ETS Editrice, Pisa, 1991), p. 99; M.A. Ol'shanii, V.G. Minogin, Opt. Commun. **89**, 393 (1992).
6. J. Lawall, F. Bardou, B. Saubamea, K. Shimizu, M. Leduc, A. Aspect, C. Cohen-Tannoudji, Phys. Rev. Lett. **73**, 1915 (1994).

7. J. Lawall, S. Kulin, B. Saubamea, N. Bigelow, M. Leduc, C. Cohen-Tannoudji, Phys. Rev. Lett. **75**, 4195 (1995).
8. M. Weidemüller, T. Esslinger, M.A. Ol'shanii, A. Hemmerich, T.W. Hänsch, Europhys. Lett. **27**, 109 (1994).
9. F. Mauri, E. Arimondo, Appl. Phys. B **54**, 420 (1992).
10. R. Dum, Phys. Rev. A **54**, 3299 (1996).
11. S. Kulin, B. Saubamea, E. Peik, J. Lawall, T.W. Hijmans, M. Leduc, C. Cohen-Tannoudji, Phys. Rev. Lett. **78**, 4185 (1997).
12. B. Saubamea, T.W. Hijmans, S. Kulin, E. Rasel, E. Peik, M. Leduc, C. Cohen-Tannoudji, Phys. Rev. Lett. **79**, 3146 (1997).
13. M.A. Ol'shanii, V.G. Minogin, Quant. Optics **3**, 317 (1991).
14. A.V. Taichenachev, A.M. Tumaikin, V.I. Yudin, M.A. Ol'shanii, Sov. Phys. JETP **74**, 952 (1992).
15. F. Papoff, F. Mauri, E. Arimondo, J. Opt. Soc. Am. B **9**, 321 (1992).
16. E. Arimondo, Laser Manipulation of Atoms and Ions, *Proceedings of the International School of Physics "Enrico Fermi"*, edited by E. Arimondo, W.D. Phillips, F. Strumia (North Holland, Elsevier Science Publishers B.V., 1991), Course CXVIII.
17. C. Cohen-Tannoudji, Les Houches, Session LIII, *Fundamental Systems in Quantum Optics*, edited by J. Dalibard, J.M. Raymond, J. Zinn-Justin (Elsevier Science Publishers B. V., 1990), Course XXX.
18. In the special case of the phase $\phi = 0$ (or π) a fourth dark state of energy 1 $E_{\rm rec}$ exists: $|\boldsymbol{\Psi}(\mathbf{r})\rangle = \mathbf{E}_1(\mathbf{r}) - \mathbf{E}_2(\mathbf{r})$.
19. However, for such an "island", the system of constraints and interference conditions has a solution when the phase $\phi = 0[\pi]$. The dark state is given for $\phi = 0$ by: $|\Psi(\mathbf{p})\rangle = (1, 1, -\mathrm{i})|p_x = n, p_y = n+1\rangle + (\mathrm{i}, \mathrm{i}, -1)|p_x = n+1, p_y = n\rangle$, where the momenta are expressed in units of $\hbar k$ and where the 3-component vectors such as $(1, 1, -\mathrm{i})$ are the internal state components in the $|g_x\rangle, |g_y\rangle, |g_z\rangle$ basis.
20. E.L. Raab, M. Prentiss, A. Cable, S. Chu, D.E. Pritchard, Phys. Rev. Lett. **59**, 2631 (1987).
21. F. Bardou, O. Emile, J.-M. Courty, C.I. Westbrook, A. Aspect, Europhys. Lett. **20**, 681 (1992).
22. R. Dum (private communication).